European Journal of Medicinal Chemistry 61 (2013) 41–48

Contents lists available at SciVerse ScienceDirect

European Journal of Medicinal Chemistry

journal homepage: http://www.elsevier.com/locate/ejmech

Original article

Evaluation of potential Myt1 kinase inhibitors by TR-FRET based binding assay

Alexander Rohe [a], Christiane Göllner [a], Kanin Wichapong [a], Frank Erdmann [a], Ghassab M.A. Al-Mazaideh [a], Wolfgang Sippl [a,b], Matthias Schmidt [a,*]

[a] Department of Medicinal Chemistry, Institute of Pharmacy, Martin-Luther-University Halle-Wittenberg, W.-Langenbeck-Str.4, 06120 Halle, Germany
[b] Freiburg Institute for Advanced Studies (FRIAS), University Freiburg, Germany

ARTICLE INFO

Article history:
Received 31 January 2012
Received in revised form
31 May 2012
Accepted 3 June 2012
Available online 12 June 2012

Keywords:
Protein kinase Myt1
Binding assay
Inhibitor
Organic synthesis
Docking

ABSTRACT

In the human cell cycle, the Myt1 kinase is a crucial regulator of the G2/M transition. Because this membrane-associated kinase is hard to obtain and assay, there is a distinct lack of data so far. Here we report the derivatization of a glycoglycerolipid which was shown previously to be active in a Myt1 activity assay. These compounds were tested in a binding assay together with a set of common kinase inhibitors against a full-length Myt1 expressed in a human cell line. Dasatinib exhibited nanomolar affinity whereas broad coverage inhibitors such as sunitinib and staurosporine derivatives did not show any effect. We also carried out docking studies for the most potent compounds allowing further insights into the inhibitor interaction of this kinase. The glycoglycerolipids showed no significant effects in the binding assay, endorsing the idea of a mechanism of action distant from the active site.

1. Introduction

The cell cycle includes two checkpoints which provide the cell with opportunities to monitor genomic integrity. These checkpoints can delay the cell cycle progress and allow cells to repair damaged DNA in order to prevent it from being passed on to daughter cells. Many cancer cell lines show deficient G1 checkpoint mechanisms, thus relying on the G2 checkpoint far more than normal cells [1,2]. For this reason, G2 checkpoint abrogation is a promising concept to damage cancerous cells in a preferential way [3]. The main feature influencing the decision to enter mitosis is a complex composed of Cdk1 and cyclin B. Cdk1 exists in a monomeric form and is inactive as a kinase. Association with cyclin B in S- and G2-phase renders the heterodimeric kinase active. Once activated, the Cdk-cyclin complex can phosphorylate hundreds of substrate proteins, finally leading to mitosis [4,5]. Cdk1/CycB is regulated by various feedback mechanisms of which inhibitory phosphorylations at Thr14 and Tyr15 by the Wee family kinases are considered essential [6]. Wee1 phosphorylates Cdk1 specifically at Tyr15 whereas Myt1 is dual-specific for Tyr15 as well as Thr14. Abrogation of the G2 checkpoint by selective inhibition of Wee1 resulted in a sensitization of p53-deficient tumor cells to DNA-damaging agents [7] and was also shown to have single-agent anti-tumor activity against sarcoma cells [8]. Indeed, pushing the cell cycle forward into mitosis might be a more effective strategy to treat cancer than stagnation of the cell cycle, though the optimal target, be it Wee1, Myt1 or another, is not yet clear [9]. Myt1 downregulation by RNA interference did not lead to a significant augmentation of doxorubicin effects. However, inhibition by a small molecule inhibitor is proposed to be a promising option because Myt1 binds Cdk1, altering equilibria and, thus, affecting G2/M transition [10]. In addition, selective Myt1 inhibitors could help analyze contributions of the various components involved in the mitotic entry network [6]. Wee1 as a soluble protein is well investigated and has been established in many kinase panels for tests of potential inhibitors (e.g. Bruyère et al. [11]). In contrast, Myt1 as a membrane associated kinase [12] is much more difficult to prepare and test.

To the best of our knowledge, full-length Myt1 has never before been tested against a set of common kinase inhibitors. Using a coupled Cdk1 – Wee kinase activity assay, Wang et al. reported the G2 checkpoint abrogator PD0166285 to be a potent ATP-competitive inhibitor [13]. This compound proved to have strong nanomolar effects on Wee1 and Myt1 in vivo and in vitro, but the inhibitor is three times more selective for Wee1 and shows, moreover, inhibitory properties against many other tyrosine kinases such as c-Src, epidermal growth factor receptor, and

Abbreviations: BCA, bicinchoninic acid; Cdk1, cyclin dependent kinase 1; CycB, cyclin B; DMSO, dimethylsulfoxide; DTT, dithiothreitol; GGL, glycoglycerolipid; HEK, human embryonic kidney; HR-MS, high resolution mass spectrometry; TR-FRET, time-resolved fluorescence resonance energy transfer.

* Corresponding author. Tel.: +49 345 55 25188; fax: +49 345 55 27018.
E-mail address: Matthias.schmidt@pharmazie.uni-halle.de (M. Schmidt).

0223-5234/$ – see front matter © 2012 Elsevier Masson SAS. All rights reserved.
http://dx.doi.org/10.1016/j.ejmech.2012.06.007

platelet-derived growth factor receptor [14,15]. A natural product originally derived from marine algae was reported to have strong inhibitory effects on Myt1 (IC_{50} 0.12 μg/ml) and, additionally, showed high selectivity over other kinases such as Akt and Chk1 [16]. Chemically, the isolated product is a glycoglycerolipid (GGL), whose scaffold is totally different from that of conventional inhibitors. We synthesized the respective GGL and performed a systematic derivatization to exclude unspecific effects and to investigate the actual mechanism.

In addition to the unknown inhibition pattern, Myt1 assay development is hindered by a restrictive substrate acceptance [17]. Therefore, we used a TR-FRET based kinase binding assay [18] to evaluate potential inhibitors.

2. Chemistry

2.1. Organic synthesis

2.1.1. Strategy

A collection of GGLs based on the reported Myt1 inhibitor was synthesized. Previously, we described the neosynthesis of 1,2-dipalmitoyl-3-(*N*-palmitoyl-6′-amino-6′-deoxy-α-D-glucosyl)-*sn*-glycerol (**1α**) in a multistep strategy starting from α-methylglucopyranoside [19]. Based on these results, we altered the hexopyranose core from the glucoside to the epimeric mannoside and galactoside with respect to the anomeric configuration. Furthermore, using the glucoside as a starting point, the palmitoyl chains were shortened to octanoyl chains. Synthesis route and conditions are displayed in Scheme 1. Briefly, the starting material was blocked in position 6 by tritylation of the primary hydroxyl group. After benzylation of the remaining secondary hydroxyl groups we removed the trityl residue to convert the 6-OH group into an azide after activation with methanesulfonyl chloride. Demethylation in position 1 led to a glycosyl donor which reacts after activation with (*S*)-1,2-isopropylideneglycerol. After hydrolysis of the ketal, the characteristic hydrophobic chains can be inserted by acylation. Reduction of the azido group yielded the respective amine that was *N*-acetylated to realize the third acyl chain. Finally, catalytic hydrogenation gave the aspired products. Identities were confirmed by NMR spectroscopic analysis and high resolution mass spectrometry (HR-MS).

A general illustration of the compounds synthesized is shown in Table 1. Characterization of intermediate products for **1α** is already described in Ref. [19]. In terms of the other final products, characterization of intermediate compounds was carried out analogously. Due to reasons of data compression we herein report data for final products only.

Mass spectra (MS) were recorded off-line with nano-ESI (Proxeon emitters, Odense, Denmark) on a LTQ-Orbitrap XL (Thermo Fisher Scientific, San Jose, USA). ^{1}H NMR and ^{13}C NMR spectra were recorded on a Varian Gemini 2000 and a Varian Inova 500; chemical shifts were referenced to residual solvent signals and reported in ppm (δ). Chromatography was performed on silica gel (Merck silica gel 60, 40–63 mesh) by MPLC. Therefore, columns were prepared with a Cartridger C-670 (Büchi). Fractions were sampled with a *Fraction Collector C*-660 (Büchi) by discontinuous enhancement of polarity, for pressure we used a Pump Module C-601 and a Pump Manager C-615 (Büchi). TLC was carried out on silica gel plates (E. Merck 60 F_{254}); spots were detected visually by ultraviolet irradiation (254 nm) or by spray detection (solution of 0.5 g thymol and 5 ml conc. sulfuric acid in 100 ml ethanol) and heated to 130 °C for 10 min. All reagents were used as purchased unless stated otherwise. Solvents were dried according to standard procedures. All reactions were carried out under an atmosphere of dry argon. All chemicals were purchased from Sigma-Aldrich (Schnelldorf, Germany).

2.1.2. Characterization of final products

*2.1.2.1. 1,2-Dipalmitoyl-3-(N-palmitoyl-6′-amino-6′-deoxy-α-D-glucosyl)-sn-glycerol (**1α**).* ^{1}H NMR: 500 MHz, $CDCl_3$: δ = 5.85–5.89 (m, 1H, –N*H*–CO–), 5.19–5.23 (m, 1H, *sn*2), 4.78 (d, 1H, $^3J_{H\text{-}1/H\text{-}2}$ = 3.7 Hz, *H*-1), 4.36 (dd, 1H, $^2J_{sn1/sn1'}$ = 11.8 Hz, $^3J_{sn1/sn2}$ = 4.0 Hz, *sn*1), 4.11 (dd, 1H, $^2J_{sn1/sn1'}$ = 11.8 Hz, $^3J_{sn1'/sn2}$ = 5.7 Hz, *sn*1′), 3.97–4.03 (m, 1H, *H*-6), 3.77 (dd, 1H, $^2J_{sn3/sn3'}$ = 10.7 Hz, $^3J_{sn2/sn3}$ = 4.4 Hz, *sn*3), 3.71 (t, 1H, ^3J = 9.4 Hz, *H*-3), 3.61 (dd, 1H, $^2J_{sn3/sn3'}$ = 10.7 Hz, $^3J_{sn3'/sn2}$ = 6.0 Hz, *sn*3′), 3.54–3.57 (m, 1H, *H*-5), 3.46 (dd, 1H, $^3J_{H\text{-}1/H\text{-}2}$ = 3.7 Hz, $^3J_{H\text{-}2/H\text{-}3}$ = 9.4 Hz, *H*-2), 3.08 (t, 1H, ^3J = 9.4 Hz, *H*-4), 3.00–3.04 (m, 1H, *H*-6′), 2.27–2.30 (m, 4H, 2× (–O–CO–CH_2–)), 2.21–2.24 (m, 2H, –NH–CO–CH_2–), 1.55–1.63 (m, 6H, 3× (–CO–CH$_2$–CH_2–(CH$_2$)$_{12}$–CH$_3$)), 1.21–1.31 (m, 72H, 3× (–CH$_2$–CH$_2$–(CH_2)$_{12}$–CH$_3$)), 0.86 (t, 9H, *J* = 7.0 Hz, 3× (–CH_3)); ^{13}C NMR: 100 MHz, $CDCl_3$: δ = 13.4, 23.1, 24.7, 25.3, 25.7, 28.5–29.8, 32.1, 33.7, 34.7, 36.9, 39.9, 62.2, 66.6, 69.8, 70.3, 71.3,72.6, 73.6, 76.8, 99.7, 172.8, 173.3, 175.4; MALDI TOF mass spectrum: *m*/*z* 990 (M + Na^+). HRFABMS *m*/*z* 968.8121 [M + H^+]; (calcd for $C_{57}H_{110}NO_{10}$ 968.8130).

*2.1.2.2. 1,2-Dipalmitoyl-3-(N-palmitoyl-6′-amino-6′-deoxy-β-D-glucosyl)-sn-glycerol (**1β**).* ^{1}H NMR: 500 MHz, $CDCl_3$: δ = 6.68–6.72 (m, 1H, –N*H*–CO–), 5.32–5.36 (m, 1H, *sn*2), 4.58 (dd, 1H, $^2J_{sn1/}$

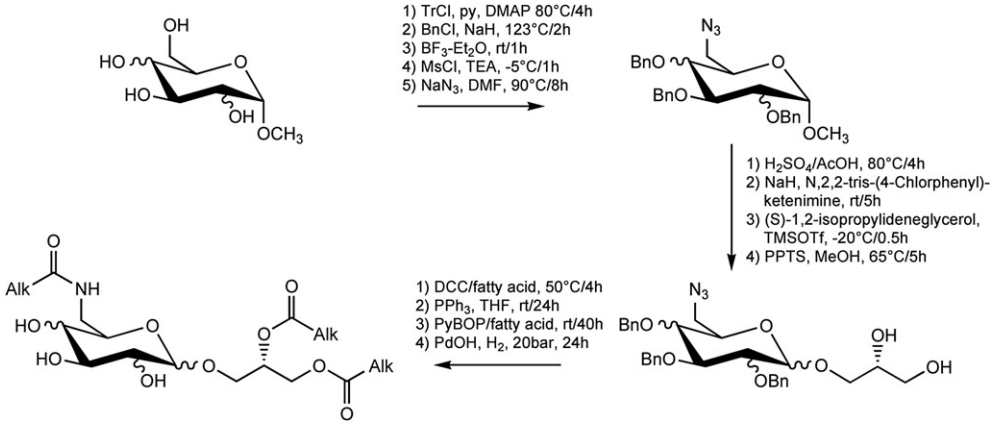

Scheme 1. General scheme of organic synthesis for the glycoglycerolipids starting from the α-methylglycoside in a 13 step synthesis route.

Table 1
Synthesized glycoglycerolipids. The sugar core was varied from glucose (**1α**, **1β**) to galactose (**2α**, **2β**) and mannose (**3α**, **3β**). Using the glucoside, octanoyl chains were inserted instead of palmitoyl chains (**4α**).

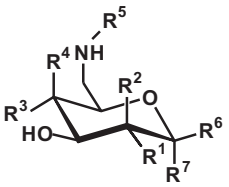

	R^1	R^2	R^3	R^4	R^5	R^6	R^7
1α	OH	H	OH	H	P[a]	H	DPG[b]
1β	OH	H	OH	H	P	DPG	H
2α	H	OH	OH	H	P	H	DPG
2β	H	OH	OH	H	P	DPG	H
3α	OH	H	H	OH	P	H	DPG
3β	OH	H	H	OH	P	DPG	H
4α	OH	H	OH	H	C[c]	H	DCG[d]

[a] P: palmitoyl.
[b] DPG: 1,2-dipalmitoyl-*sn*-glycerol.
[c] C: capryloyl.
[d] DCG: 1,2-dicapryloyl-*sn*-glycerol.

$_{sn1'}$ = 11.9 Hz, $^3J_{sn1/sn2}$ = 3.4 Hz, *sn*1), 4.32 (d, 1H, $^3J_{H\text{-}1/H\text{-}2}$ = 7.6 Hz, *H*-1), 3.99–4.11 (m, 2H, *H*-6, *sn*1′), 3.74–3.83 (m, 2H, *sn*3, *sn*3′), 3.57 (t, 1H, ^3J = 9.2 Hz, *H*-3), 3.35 (t, 1H, ^3J = 9.2 Hz, *H*-2), 3.22–3.27 (m, 1H, *H*-5), 3.13 (t, 1H, ^3J = 9.2 Hz, *H*-4), 3.04–3.09 (m, 1H, *H*-6′), 2.23–2.33 (m, 6H, 3× (−O−CO−C*H*$_2$−)), 1.50–1.63 (m, 6H, 3× (−CO−CH$_2$−C*H*$_2$−(CH$_2$)$_{12}$−CH$_3$)), 1.20–1.31 (m, 72H, 3× (−CH$_2$−CH$_2$−(C*H*$_2$)$_{12}$−CH$_3$)), 0.86 (t, 9H, *J* = 6.7 Hz, 3× (−C*H*$_3$)); ^{13}C NMR: 100 MHz, CDCl$_3$: δ = 13.1, 23.4, 24.6, 25.2, 25.8, 28.3–29.7, 32.2, 33.5, 34.8, 36.7, 40.0, 62.1, 66.3, 69.6, 70.1, 71.4, 72.4, 73.5, 76.7, 99.3, 172.9, 173.3, 175.1; MALDI TOF mass spectrum: *m*/*z* 990 (M + Na$^+$). HRFABMS *m*/*z* 968.81242 [M + H$^+$]; (calcd for $C_{57}H_{110}NO_{10}$ 968.8130).

*2.1.2.3. 1,2-Dipalmitoyl-3-(N-palmitoyl-6′-amino-6′-deoxy-α-D-mannosyl)-sn-glycerol (**2α**).* ^{1}H NMR: 500 MHz, CDCl$_3$: δ = 6.04–6.07 (m, 1H, −N*H*−CO−), 5.15–5.18 (m, 1H, *sn*2), 4.77 (s, 1H, *H*-1), 4.30 (dd, 1H, $^2J_{sn1/sn1'}$ = 11.7 Hz, $^3J_{sn1/sn2}$ = 3.9 Hz, *sn*1), 4.10 (dd, 1H, $^2J_{sn1/sn1'}$ = 11.7 Hz, $^3J_{sn1'/sn2}$ = 5.9 Hz, *sn*1′), 4.01–4.06 (m, 1H, *H*-6), 3.95 (d, 1H, ^3J = 2.6 Hz, *H*-2), 3.84 (dd, 1H, $^3J_{H\text{-}2/H\text{-}3}$ = 2.9 Hz, $^3J_{H\text{-}3/H\text{-}4}$ = 9.3 Hz, *H*-3), 3.73 (dd, 1H, $^2J_{sn3/sn3'}$ = 10.7 Hz, $^3J_{sn2/sn3}$ = 4.9 Hz, *sn*3), 3.56 (dd, 1H, $^2J_{sn3/sn3'}$ = 10.7 Hz, $^3J_{sn2/sn3}$ = 5.4 Hz, *sn*3′), 3.50–3.53 (m, 1H, *H*-5), 3.43 (t, 1H, ^3J = 9.3 Hz, *H*-4), 2.98–3.03 (m, 1H, *H*-6′), 2.22–2.30 (m, 6H, 3× (−CO−C*H*$_2$−)), 1.55–1.64 (m, 6H, 3× (−CO−CH$_2$−C*H*$_2$−(CH$_2$)$_{12}$−CH$_3$)), 1.21–1.30 (m, 72H, 3× (−CH$_2$−CH$_2$−(C*H*$_2$)$_{12}$−CH$_3$)), 0.86 (t, 9H, *J* = 6.8 Hz, 3× (−C*H*$_3$)); ^{13}C NMR: 100 MHz, CDCl$_3$: δ = 13.3, 23.2, 24.8, 25.2, 25.7, 28.5–29.7, 32.3, 33.6, 34.9, 36.4, 39.7, 62.0, 66.4, 69.7, 70.0, 71.1,72.5, 73.5, 76.8, 99.6, 172.5, 173.7, 175.2; MALDI TOF mass spectrum: *m*/*z* 990 (M + Na$^+$). HRFABMS *m*/*z* 990.7900 [M + Na$^+$]; (calcd for $C_{57}H_{109}NaNO_{10}$ 990.7949).

*2.1.2.4. 1,2-Dipalmitoyl-3-(N-palmitoyl-6′-amino-6′-deoxy-β-D-mannosyl)-sn-glycerol (**2β**).* ^{1}H NMR: 500 MHz, CDCl$_3$: δ = 6.69–6.73 (m, 1H, −N*H*−CO−), 5.30–5.34 (m, 1H, *sn*2), 4.55 (dd, 1H, $^2J_{sn1/sn1'}$ = 12.1 Hz, $^3J_{sn1/sn2}$ = 2.9 Hz, *sn*1), 4.50 (s, 1H, *H*-1), 3.96–4.07 (m, 3H, *H*-2, *H*-6, *sn*1′), 3.76–3.84 (m, 2H, *sn*3, *sn*3′), 3.59 (dd, 1H, $^3J_{H\text{-}2/H\text{-}3}$ = 2.6 Hz, $^3J_{H\text{-}3/H\text{-}4}$ = 9.5 Hz, *H*-3), 3.48 (t, 1H, ^3J = 9.5 Hz, *H*-4), 3.12–3.18 (m, 2H, *H*-5, *H*-6′), 2.24–2.32 (m, 6H, 3× (−CO−C*H*$_2$−)), 1.55–1.64 (m, 6H, 3× (−CO−CH$_2$−C*H*$_2$−(CH$_2$)$_{12}$−CH$_3$)), 1.20–1.31 (m, 72H, 3× (−CH$_2$−CH$_2$−(C*H*$_2$)$_{12}$−CH$_3$)), 0.86 (t, 9H, *J* = 7 Hz, 3× (−C*H*$_3$)); ^{13}C NMR: 100 MHz, CDCl$_3$: δ = 13.8, 23.3, 24.5, 25.6, 25.9, 28.8–29.6, 31.9, 33.4, 34.5, 36.7, 39.8, 61.8, 66.1, 69.7, 70.2, 71.4, 72.5, 73.6, 76.7, 99.9, 172.5, 173.7, 175.2; MALDI TOF mass spectrum: *m*/*z* 990 (M + Na$^+$). HRFABMS *m*/*z* 990.79492 [M + Na$^+$]; (calcd for $C_{57}H_{109}NaNO_{10}$ 990.7949).

*2.1.2.5. 1,2-Dipalmitoyl-3-(N-palmitoyl-6′-amino-6′-deoxy-α-D-galactosyl)-sn-glycerol (**3α**).* ^{1}H NMR: 500 MHz, CDCl$_3$: δ = 5.90–5.93 (m, 1H, −N*H*−CO−), 5.21–5.25 (m, 1H, *sn*2), 4.86 (d, 1H, $^3J_{H\text{-}1/H\text{-}2}$ = 3.4 Hz, *H*-1), 4.30 (dd, 1H, $^2J_{sn1/sn1'}$ = 11.7 Hz, $^3J_{sn1/sn2}$ = 3.4 Hz, *sn*1), 4.11 (dd, 1H, $^2J_{sn1/sn1'}$ = 11.7 Hz, $^3J_{sn1'/sn2}$ = 5.9 Hz, *sn*1′), 3.64–3,85 (m, 7H, *H*-2, *H*-3, *H*-4, *H*-5, *H*-6, *sn*3, *sn*3′), 3.08–3.13 (m, 1H, *H*-6′), 2.28–2.32 (m, 4H, 2× (−O−CO−C*H*$_2$−)), 2.18 (t, 2H, *J* = 7.3 Hz, −NH−CO−C*H*$_2$−), 1.55–1.62 (m, 6H, 3× (−CO−CH$_2$−C*H*$_2$−(CH$_2$)$_{12}$−CH$_3$)), 1.21–1.30 (m, 72H, 3× (−CH$_2$−CH$_2$−(C*H*$_2$)$_{12}$−CH$_3$)), 0.86 (t, 9H, *J* = 7.3 Hz, 3× (−C*H*$_3$)); ^{13}C NMR: 100 MHz, CDCl$_3$: δ = 13.5, 23.5, 24.6, 25.1, 25.6, 28.4–29.7, 32.0, 33.7, 34.7, 36.8, 39.6, 62.0, 66.3, 69.9, 70.7, 71.1, 72.4, 73.8, 76.6, 99.7, 172.7, 173.3, 175.4; MALDI TOF mass spectrum: *m*/*z* 990 (M + Na$^+$). HRFABMS *m*/*z* 968.8125 [M + H$^+$]; (calcd for $C_{57}H_{110}NO_{10}$ 968.8130).

*2.1.2.6. 1,2-Dipalmitoyl-3-(N-palmitoyl-6′-amino-6′-deoxy-β-D-galactosyl)-sn-glycerol (**3β**).* ^{1}H NMR: 500 MHz, CDCl$_3$: δ = 6.28–6.32 (m, 1H, −N*H*−CO−), 5.25–5.30 (m, 1H, *sn*2), 4.35 (dd, 1H, $^2J_{sn1/sn1'}$ = 11.9 Hz, $^3J_{sn1/sn2}$ = 2.1 Hz, *sn*1), 4.19–4.22 (m, 2H, *H*-1, *sn*1′), 3.80–3.86 (m, 3H, *H*-4, *H*-6, *sn*3), 3.73 (dd, 1H, $^2J_{sn3/sn3'}$ = 10.7 Hz, $^3J_{sn2/sn3'}$ = 6.7 Hz, *sn*3′), 3.57–3.61 (m, 1H, *H*-2), 3.54 (dd, 1H, $^3J_{H\text{-}2/H\text{-}3}$ = 9.2 Hz, $^3J_{H\text{-}3/H\text{-}4}$ = 2.1 Hz, *H*-3), 3.47–3.50 (m, 1H, *H*-5), 3.24–3.29 (m, 1H, *H*-6′), 2.27–2.32 (m, 4H, 2× (−O−CO−C*H*$_2$−)), 2.22 (t, 2H, *J* = 7.3 Hz, −NH−CO−C*H*$_2$−), 1.56–1.62 (m, 6H, 3× (−CO−CH$_2$−C*H*$_2$−(CH$_2$)$_{12}$−CH$_3$)), 1.20–1.31 (m, 72H, 3× (−CH$_2$−CH$_2$−(C*H*$_2$)$_{12}$−CH$_3$)), 0.86 (t, 9H, *J* = 7 Hz, 3× (−C*H*$_3$)); ^{13}C NMR: 100 MHz, CDCl$_3$: δ = 13.8, 23.2, 24.7, 25.3, 25.7, 28.5–29.8, 32.2, 32.7, 34.3, 36.9, 39.9, 62.2, 66.6, 69.8, 70.3, 71.3,72.6, 73.6, 76.8, 99.6, 172.5, 173.4, 175.1; MALDI TOF mass spectrum: *m*/*z* 990 (M + Na$^+$). HRFABMS *m*/*z* 990.79577 [M + Na$^+$]; (calcd for $C_{57}H_{109}NaNO_{10}$ 990.7949).

*2.1.2.7. 1,2-Diocteoyl-3-(N-octeoyl-6′-amino-6′-deoxy-α-D-glucosyl)-sn-glycerol (**4α**).* ^{1}H NMR: 500 MHz, CDCl$_3$: δ = 5.88–5.93 (m, 1H, −CH$_2$−N*H*−CO−), 5.19–5.23 (m, 1H, *sn*2), 4.78 (d, 1H, $^3J_{H\text{-}1/H\text{-}2}$ = 4 Hz, *H*-1), 4.36 (dd, 1H, $^2J_{sn1/sn1'}$ = 11.9 Hz, $^3J_{sn1/sn2}$ = 4 Hz, *sn*1), 4.11 (dd, 1H, $^2J_{sn1/sn1'}$ = 11.9 Hz, $^3J_{sn1'/sn2}$ = 5.9 Hz, *sn*1′), 3.99 (ddd, 1H, $^3J_{H\text{-}5/H\text{-}6}$ = 2.6 Hz, $^3J_{-NH-/H\text{-}6}$ = 8.2 Hz, $^2J_{H\text{-}6/H\text{-}6'}$ = 15 Hz, *H*-6), 3.77 (dd, 1H, $^2J_{sn3/sn3'}$ = 11 Hz, $^3J_{sn2/sn3}$ = 4.8 Hz, *sn*3), 3.71 (t, 1H, ^3J = 9.5 Hz, *H*-3), 3.61 (dd, 1H, $^2J_{sn3/sn3'}$ = 11 Hz, $^3J_{sn2/sn3'}$ = 5.9 Hz, *sn*3′), 3.56 (ddd, 1H, $^3J_{H\text{-}4/H\text{-}5}$ = 9.5 Hz, $^3J_{H\text{-}5/H\text{-}6'}$ = 2.6 Hz, $^3J_{H\text{-}5/H\text{-}6}$ = 2.9 Hz, *H*-5), 3.46 (dd, 1H, $^3J_{H\text{-}1/H\text{-}2}$ = 4.0 Hz, $^3J_{H\text{-}2/H\text{-}3}$ = 9.5 Hz, *H*-2), 3.08 (t, 1H, ^3J = 9.5 Hz, *H*-4), 3.03 (ddd, 1H, $^3J_{H\text{-}5/H\text{-}6'}$ = 2.9 Hz, $^3J_{-NH-/H\text{-}6'}$ = 4.4 Hz, $^2J_{H\text{-}6/H\text{-}6'}$ = 15 Hz, *H*-6′), 2.60 (bs, 3H, 3× (−O*H*)), 2.27–2.31 (m, 4H, 2× (−CO−C*H*$_2$−(CH$_2$)$_5$−CH$_3$)), 2.21–2.24 (m, 2H, −NH−CO−C*H*$_2$−(CH$_2$)$_5$−CH$_3$), 1.56–1.64 (m, 6H, 3× (−CH$_2$−C*H*$_2$−(CH$_2$)$_4$−CH$_3$)), 1.22–1.30 (m, 24H, 3× (−(CH$_2$)$_2$−(C*H*$_2$)$_4$−CH$_3$), 0.84–0.87 (m, 9H, 3× (−C*H*$_3$)); ^{13}C NMR: 100 MHz, CDCl$_3$: δ = 14.0, 22.6, 24.8, 24.9, 25.6, 28.9–29.7, 31.6, 34.1, 34.2, 36.4, 39.8, 62.1, 66.9, 69.9, 70.1, 71.1, 72.4, 73.1, 76.7, 99.4, 173.2, 173.4, 175.7; MALDI TOF mass spectrum: *m*/*z* 655 (M + Na$^+$). HRFABMS *m*/*z* 654.41877 [M + Na$^+$]; (calcd for $C_{33}H_{61}NaNO_{10}$ 654.4193).

2.2. Computational chemistry: ligand preparation and molecular docking study

All ligands were constructed using MOE2010.10 [20] and energy minimized using the MMFF94 force field with a convergence

criteria of 0.01 kcal/mol. The protonation state of the ligand was assigned at pH 7.1 using the protonated-3D module implemented in MOE2010.10. Dasatinib and PD0166285 were docked into the binding pocket of the X-ray structure of a truncated Myt1 (PDB code 3P1A, active form of Myt1) using GOLD version 5.0 [21,22]. According to our previous studies [23,24], GOLD is able to correctly predict the binding mode of Wee1 kinase inhibitors. Moreover, we were able to dock the pyridopyrimidine derivatives, which have the same scaffold as PD0166285, into the binding pocket of Wee1 kinase [23]. Since Wee1 and Myt1 show a high structural similarity, we used the same protocol as applied for Wee1 kinase docking for Myt1 kinase docking. We defined Cys190 located at the hinge region as center of the binding site with a radius of 20 Å. Beside free docking we tested also the influence of protein hydrogen bond constraints to the hinge region residues Glu188 and Cys190 (backbone heteroatoms). Water molecules found at the binding pocket of Myt1 were also applied for docking using 'toggle' mode in GOLD.

3. Results

3.1. Set of common kinase inhibitors

Because common kinase inhibitors have not been tested on human Myt1 kinase so far, we used known pan-kinase inhibitors such as staurosporine as well as more selective tyrosine kinase inhibitors which have been approved and marketed such as lapatinib and imatinib to obtain a first inhibition profile.

All compounds were tested three times at two different concentrations. Any substance binding >50% at 10 μM was subjected to further testing and IC_{50} values were determined. Quantitative data is expressed as mean ± standard error. Curves were fitted to the data by GraphPad Prism 5.01 (San Diego, CA) using sigmoidal dose response with a variable slope. PD0166285 (**5**) was used as a positive control. Compounds and respective effects at a concentration as indicated are displayed in Table 2.

Most of the tested compounds did not affect Myt1. The kinase was insensitive even towards highly promiscuous inhibitors such as staurosporine and bisindolylmaleimide I. The effects of erlotinib and gefitinib were negligible. Major effects could be determined for dasatinib (**7**) and tyrphostin AG 1478 (**6**). However, binding of the latter was too weak to determine IC_{50} values due to limitations of the assay system (see Discussion). Dasatinib bound to Myt1 with an IC_{50} of about 63 nM (Fig. 1).

The positive control PD0166285 had an IC_{50} of 7.1 nM in this assay. The chemical structures of compounds which affected Myt1 are shown in Fig. 2. The scaffold of PD0166285 and tyrphostin AG 1478 show a high degree of similarity.

The potent inhibitors were subjected to further in silico studies to investigate their potential interaction at the kinase binding site.

Table 2
Test of common kinase inhibitors for effects on human full-length Myt1 kinase. Binding of the respective compound is reported in [relative % tracer displaced].

Compound	Displacement [%] at 5 μM	Displacement [%] at 10 μM	IC_{50} [nM]
Bisindolyl-maleimide I	n.d.[a]	n.d.	n.t.[b]
Dasatinib	95.5 ± 0.3	97.1 ± 0.3	63.0 ± 1.1
Erlotinib	7.05 ± 1.65	8.15 ± 0.65	n.t.
Gefitinib	n.d.	6.85 ± 2.35	n.t.
HA-1077	n.d.	n.d.	n.t.
Imatinib	n.d.	n.d.	n.t.
K252a	n.d.	n.d.	n.t.
Lapatinib	n.d.	n.d.	n.t.
PD0166285	n.t.	n.t.	7.2 ± 1.1
Midostaurin	n.d.	n.d.	n.t.
SB 203580	n.d.	n.d.	n.t.
Staurosporine	n.t.	n.t.	n.d. up to 10 μM
Sunitinib	n.d.	n.d.	n.t.
Tyrphostin AG 1478	24.8 ± 0.7	39.5 ± 1.5	n.t.
U0126	7.55 ± 0.65	n.d.	n.t.
Vatalanib	n.d.	n.d.	n.t.

[a] n.d.: no displacement (<5%) at the specified assay concentration.
[b] n.t.: not tested.

3.2. Docking studies

3.2.1. Examination of the Myt1 ATP binding pocket

We first analyzed the X-ray structure of Myt1 (PDB Code 3P1A) and Wee1 (PDB code 1X8B). Even though the sequence identity between Wee1 and Myt1 is rather low (35.3%) [17], the overall 3D-structures, especially the binding pocket, are quite similar as shown in Fig. 3.

Root mean square deviation (RMSD) between these two structures is 1.73 Å (backbone atoms). Therefore, it is reasonable to use the same protocol for Myt1 docking as for Wee1 docking. As discussed previously [24], the X-ray structures of Wee1-inhibitor complexes reveal the interaction between inhibitors and the residues Glu377 and Cys379 located at the hinge region. It is well known from other kinases that the residues at the hinge region play an important role for interacting with ATP-competitive inhibitors or ATP. Thus, the key residues where inhibitors and ATP bind are Glu188, Cys190 and the gatekeeper residue of Myt1 (Thr187) as displayed in Fig. 3.

3.2.2. Molecular docking

In our previous work [23], we were able to dock the pyridopyrimidine derivatives into the binding pocket of Wee1 kinase. The docking results showed a conserved binding, namely an H-bond interaction between the NH and N atom of the inhibitor's pyrimidine ring (the main scaffold) with the Cys379 residue. For the Myt1 kinase, the docking also showed the same binding mode, as displayed in Fig. 4A. The H-bond interactions were found between the NH atom and the pyrimidine ring of the inhibitor with Cys190. The benzene ring with the chloro substituent at the ortho position is located at the hydrophobic pocket. There is also another interaction between the benzene ring of the inhibitor with Pro192 and Leu116, as shown in Fig. 4B.

Dasatinib is a well-known kinase inhibitor, and several X-ray structures of kinases (active conformation) complexed with dasatinib are available in the Protein Data Bank; for example PDB code 2GQG (Abl kinase), 3G5D (c-Src kinase), and 3K54 (Btk kinase).

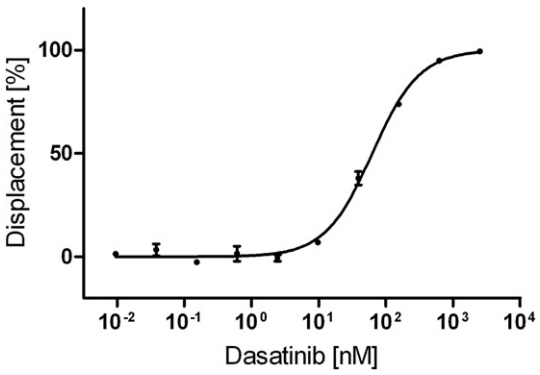

Fig. 1. Binding of dasatinib to Myt1. Data expressed as mean ± standard error and reported in [relative % tracer displaced]. The IC_{50} was determined 63.0 ± 1.1 nM.

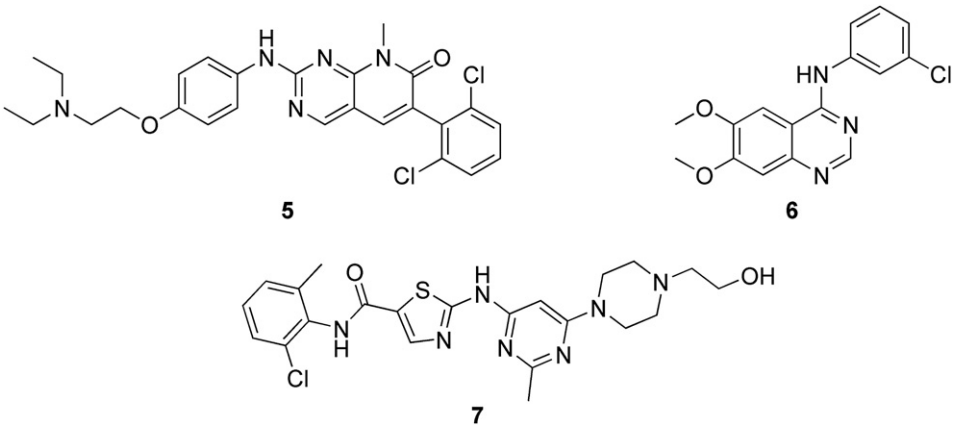

Fig. 2. Chemical structures of the compounds affecting Myt1 in a significant manner: **5** (PD0166285), **6** (Tyrphostin AG 1478) and **7** (Dasatinib).

Superimposition of these X-ray structures (Fig. 5) reveals that dasatinib not only forms H-bonds with residues at the hinge region but also with the gatekeeper residue.

Our molecular docking results for dasatinib and Myt1 (PDB code 3P1A, active conformation) as displayed in Fig. 6A also yielded the same binding mode as for the other protein kinases. H-bond interactions were found between NH and the N atom of the thiazole ring with Cys190, and between the NH atom with Thr186 (gatekeeper residue for Myt1). The additional interaction between dasatinib and Pro192 were also found as shown in Fig. 6B.

3.3. Biological evaluation of the glycoglycerolipids

The GGLs were tested three times in the kinase binding assay at 3 μg/ml and 30 μg/ml. Table 3 summarizes the results.

No effects on Myt1 could be determined. Only **2α** showed a negligible displacement of the kinase tracer at 30 μg/ml.

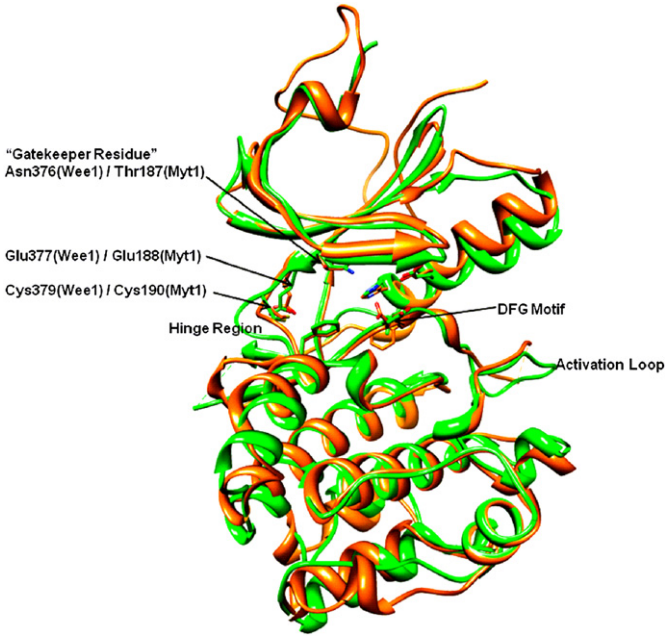

Fig. 3. Comparison of the overall structure of Wee1 (PDB Code 1X8B) and Myt1 (PDB Code 3P1A). The structure of Wee1 and Myt1 are shown as green and orange ribbon, respectively. (For interpretation of the references to colour in this figure legend, the reader is referred to the web version of this article.)

4. Discussion

The restrictive substrate acceptance of the human Myt1 kinase led us to use a binding assay instead of an activity assay. In general, the use of binding assays in drug discovery is not necessarily accompanied by disadvantages. It has been shown that data gained by a kinase binding assay may provide a better correlation to cellular effects than a conventional enzyme activity assay. Moreover, the identification of hits targeting inactive kinase conformations is strongly facilitated compared to activity assays [18,25].

Even the largest available kinase panels contain only a fraction of all 518 kinases of the human kinome, and often the kinase domain only instead of the full-length protein. In addition, the panels are often highly biased by containing mostly kinases that can be easily purified and assayed. Additionally, as these kinases are typically purified from non-mammalian cells, they do not contain their naturally occurring post-translational modifications [26]. We provide data for a difficult to obtain membrane-associated kinase which is, to our best knowledge, not commercially available as an enzymatically active protein. This kinase is of special interest because it is involved in pathways of major importance for development and survival of many cancer cells.

Staurosporine was found not to bind to Myt1. This result supports a recent study with the Myt1 kinase domain which was expressed in *E. coli* [27] and is, furthermore, cross-validated by the fact that the staurosporine derivatives midostaurin and K252a did not show any effect in concentrations up to 10 μM either. Also other compounds which usually inhibit a broad range of kinases (e.g. sunitinib) did not affect Myt1. Because assay development requires positive controls, i.e. known inhibitors, these unusual inhibition properties may be jointly responsible for the lack of data so far. Higher concentrations of negative compounds could not be tested because autofluorescent compounds can serve as FRET acceptors via a non-specific diffusion enhanced FRET mechanism and therefore interfere by increased background signal and narrowed assay window [18,28]. According to our experience, the presence of compounds containing aromatic systems, as are present in most kinase inhibitors, is therefore limited to about 10 μM.

Myt1 was expressed in a human cell line, which means any posttranslational modifications are approximately as in the actual human target cells. The tested kinase preparation showed catalytic activity towards Thr14 and Tyr15 of Cdk1 [17]. Additionally, due to the fact that the epitope tag is present in the kinase of interest only, the assay system used is insensitive to contaminating kinases. Together with the affirmation of PD0166285 as a tightly binding compound, our results appear valid. Previously, Myt1 was

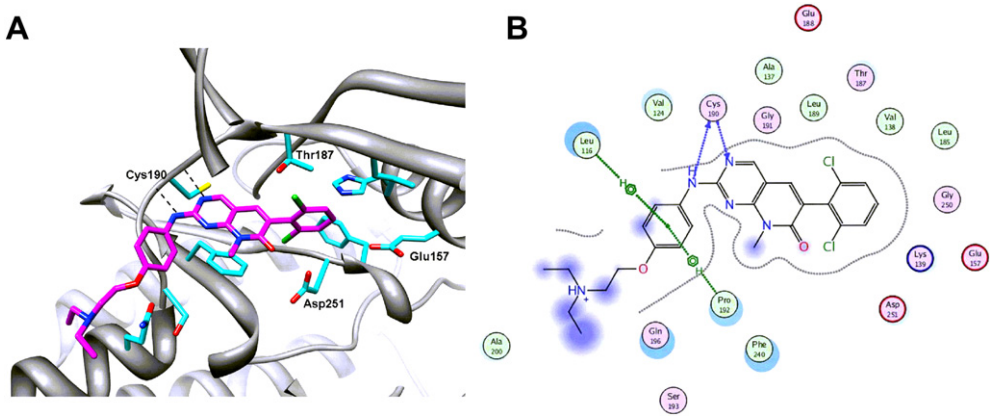

Fig. 4. (A) GOLD docking solution of compound PD0166285 (magenta stick) in the binding pocket of Myt1 (B) Schematic representation of the interactions between compound PD0166285 with the residues at the binding pocket of Myt1. H-bonds are displayed as dashed lines. (For interpretation of the references to color in this figure legend, the reader referred to the web version of this article.)

suggested as a target of dasatinib using an MS-driven proteomics approach [29]. However, this approach used a chemically altered, immobilized dasatinib-derivative. Taking into account that former comparable studies did not reveal Myt1 to be a target of dasatinib [30], affirmation in a more specific way was needed. In our in vitro test system, we found dasatinib to affect Myt1 strongly, with an IC_{50} value of about 63 nM, leading to the conclusion that Myt1 may indeed be a target of dasatinib. However, the affinity of dasatinib towards its reported primary targets, Abl and Src, lying in the subnanomolar range [31], is much higher compared to Myt1. Future work has to reveal whether Myt1 can be confirmed as a substantial target also in cellular systems.

According to their binding modes, both potent inhibitors exploit a hydrophobic pocket beyond the gatekeeper residue and not only the regions targeted by ATP, favored by the small threonine residue in this position. About 18% of all protein kinases contain a Thr-gatekeeper. As this residue is not very bulky, it provides the possibility to target the backpocket in a more specific way [32]. Therefore, systematic structure activity relationship studies are needed to realize a compound providing both affinity and selectivity.

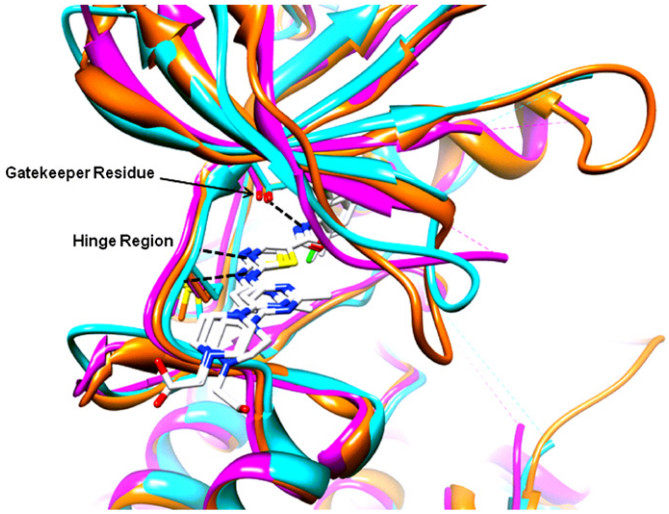

Fig. 5. Comparison of the binding mode of dasatinib (white stick) in the binding pocket of different kinases (Abl: orange-2GQG, c-Src: magenta-3G5D, and Btk: cyan-3K54). (For interpretation of the references to color in this figure legend, the reader referred to the web version of this article.)

Type III kinase inhibitors are compounds that bind exclusively to sites other than the ATP-binding site. Due to steric reasons caused by three fatty acid chains in the GGLs, a mechanism of action outside the ATP-binding site is likely, making it Type III instead of ATP-competitive. Even though most type III inhibitors do not directly bind to the ATP site, the majority must either alter the active site in a way that displaces the tracer or bind close to the active site. The GGLs did not displace the tracer, although a maximum concentration up to 250-fold the reported IC_{50} was used. Considering the potency of **1**α in an activity assay, the conclusion can be drawn that the effect of this class is unfolded distant from the active site. So far, there is only one known example of a type III inhibitor which could not be detected in the binding assay but in an activity assay. This compound inhibited p38α depending on the substrate used [33,34]. The chemical structure of the GGLs together with the cellular localization of Myt1, membrane-bound at the endoplasmic reticulum, give rise to another thesis. All tested GGLs are very hydrophobic and therefore practically insoluble in water. Not until solutizer (30% DMSO) or tenside were added could the compound be dissolved. Therefore, these compounds are likely to interact with more hydrophobic structures such as bilayers (membranes) and micelles. As can be seen in Fig. 7, the membrane association motif within the Myt1 protein sequence shows spatial proximity to both the kinase domain and the Cdk1 interaction site [35].

Because an interaction of the GGLs with the kinase domain was not observed in our study, GGL effects on the substrate (Cdk1) recognition of Myt1 might be responsible for their reported strong inhibitory potential. The lone available crystal structure of Myt1 resolves the kinase domain only, which precludes further structural studies.

From this point of view it is not surprising that the derivatized GGLs also did not show a significant effect on Myt1, though these results increase the validity of the study. However, a retest of these compounds in an activity-based assay in future work is desirable to investigate structure activity relationships and to learn about the actual mechanism of action.

5. Conclusion

A first inhibitor profile for full-length human Myt1 was provided and showed that Myt1 is quite hard to affect but, if so, the compounds are far from being selective. The glycoglycerolipids as potentially selective inhibitors are a second class of described compounds which show a discrepancy between activity assay and

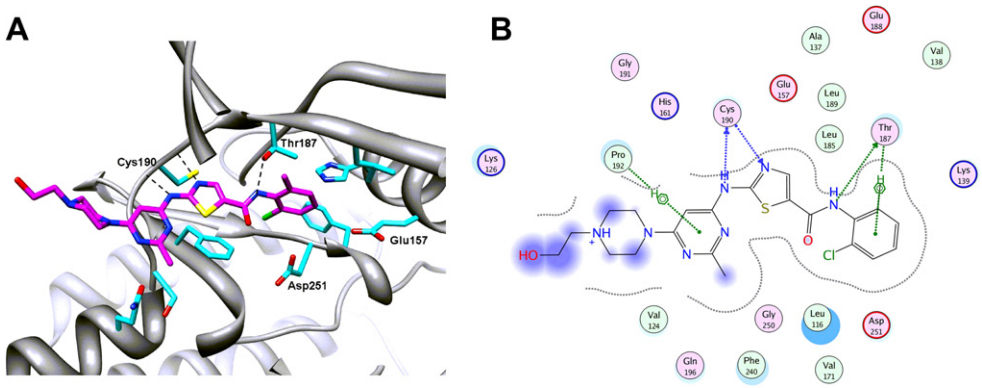

Fig. 6. (A) GOLD docking solution of dasatinib (magenta stick) in the ATP-binding pocket of Myt1. (B) Schematic representation of the interactions between dasatinib and the residues at the ATP-binding pocket of Myt1. (For interpretation of the references to color in this figure legend, the reader referred to the web version of this article.)

Table 3
Binding assay results of synthesized glycoglycerolipids for effect on human Myt1.

Compound	Displacement [%] at 3 μg/ml	Displacement [%] at 30 μg/ml
1α	n.d.	n.d.
1β	n.d.	n.d.
2α	n.d.	7.53 ± 0.04
2β	n.d.	n.d.
3α	n.d.	n.d.
3β	n.d.	n.d.
4α	n.d.	n.d.

n.d.: no displacement (<5%) at the specified assay concentration.

binding assay. This fact emphasizes that they do not target the ATP-site and also shows that this entire class should be evaluated in future activity assays. The discovery of selective Myt1 inhibitors will be of major importance to assess druggability of Myt1 and its actual role in cells. Binding mode insights provided here may help to develop such compounds by computer-aided drug design.

6. Experimental protocols

6.1. Kinase expression and purification

In this study, full-length Myt1 was expressed in the human cell line HEK293. Cells were cultured in Dulbecco's modified eagle medium (DMEM), supplemented with 10% FCS and GlutaMAX at 37 °C in a humidified incubator. Transfection was carried out with pcDNA3.1-His-Myt1 expression plasmid using lipofectamine 2000 (Invitrogen) according to recommendations of the supplier. Cells were harvested and resuspended in lysis buffer containing 25 mM Tris–HCl pH 7.8, 150 mM NaCl, 10 mM $MgCl_2$, 10% glycerol, 1% Triton X-100 and Complete EDTA-free protease inhibitor cocktail (Roche, Basel, Switzerland). Cells were finally lysed by shear stress using a 25 g needle and the lysate shaken on ice for 1 h. After centrifugation at 10 000 *g* for 15 min, the supernatant was loaded onto a HIS-Select column (Sigma) pre-equilibrated with buffer A (50 mM Tris–HCl pH 7.8; 150 mM NaCl; 3 mM $MgCl_2$; 20% glycerol; 0.5% Triton X-100). The column was washed with buffer B (buffer A + 5 mM Imidazole) and eluted with buffer C (buffer A + 250 mM Imidazole). All Steps were carried out at 4 °C and the final eluate

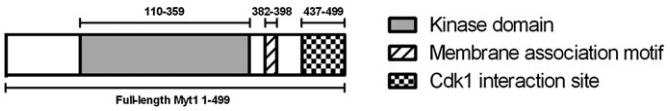

Fig. 7. Illustration of the full-length Myt1 sequence and respective function of selected regions. The membrane association motif provides spatial proximity to the kinase domain as well as the Cdk1 interaction site, rendering both functional regions possible sites of action for the glycoglycerolipids.

was supplemented with DTT (2 mM), frozen in ethanol/dry ice and stored at −80 °C. The purification was controlled by coomassie stained SDS-PAGE analysis of all fractions. Determination of protein concentrations was conducted via BCA-assay as described previously using BSA as protein standard [36]. Identity of Myt1 was additionally proven via western blotting experiments (antibody #4282; Cell Signaling).

6.2. Binding assay

Tracer and Eu-labeled antibody used in this study were from Invitrogen (Madison, WI, USA). Binding assays were performed in 384-well low volume plates (Optiplate #6007290, Perkin Elmer) at room temperature in sterile filtered kinase buffer consisting of 50 mM HEPES (pH 7.5), 0.01% Brij-35, 10 mM $MgCl_2$, and 1 mM EGTA. For all experiments with a kinase inhibitor, a dilution series of inhibitor was first prepared in 100% DMSO at 100-fold the desired final assay concentration. From this master dilution series, inhibitors were diluted 33.3-fold into kinase buffer, for an intermediate concentration of inhibitor 3-fold of that to be used in the assay (containing 3% DMSO). To 5 μl of each concentration of inhibitor to be tested, appropriate assay reagents (15 nM Myt1, 10 nM tracer, 2 nM Eu-labeled anti-His-tag antibody) were added to bring the final volume to 15 μl and the final DMSO concentration to 1%. In general, all assays were performed with 3 replicates of each inhibitor concentration. Assay plates were read using a Perkin Elmer EnVision plate reader together with standard Eu-based TR-FRET settings with 340 nm excitation wavelength and emission monitored at 615 nm (donor) and 665 nm (acceptor). Emission intensities were measured over a 100 μs window following a 60 μs postexcitation delay. A ratio of raw acceptor/donor was calculated and normalized relative to wells containing fully bound or fully competed tracer (results reported in relative percent tracer displaced). PD0166285 was purchased from Santa Cruz Biotechnology (Santa Cruz, CA, USA), Vatalanib and Erlotinib were from ChemieTek (Indianapolis, IN, USA), all other kinase inhibitors were obtained from LC Laboratories (Woburn, MA, USA). Sunitinib was a kind gift from Pfizer (Groton, CT, USA). Curve fitting and data analysis were carried out using GraphPad Prism software (GraphPad Software, Inc., La Jolla, CA, USA).

Author contribution

Alexander Rohe: In vitro tests, kinase expression and purification, preparation of manuscript. Christiane Göllner: Organic synthesis, preparation of manuscript. Kanin Wichapong: Molecular modeling, preparation of the manuscript. Frank Erdmann: Kinase

expression and purification. Ghassab M. A. Al-Mazaideh: Organic synthesis. Wolfgang Sippl: Supervision, research planning, preparation of manuscript. Matthias Schmidt: Organic synthesis, supervision, research planning, preparation of manuscript.

Acknowledgment

This work was supported by research funds from "Kultusministerium des Landes Sachsen-Anhalt". We thank Pfizer for providing sunitinib. We thank Prof. Manfred Jung from the Albert-Ludwigs-University Freiburg i. Br. for instrumentational support.

Appendix A. Supplementary data

Supplementary data associated with this article can be found in the online version, at http://dx.doi.org/10.1016/j.ejmech.2012.06.007. These data include MOL files and InChiKeys of the most important compounds described in this article.

References

[1] M. Suganuma, T. Kawabe, H. Hori, T. Funabiki, T. Okamoto, Sensitization of cancer cells to DNA damage-induced cell death by specific cell cycle G2 checkpoint abrogation, Cancer Res. 59 (1999) 5887–5891.
[2] A.J. Levine, p53, The cellular gatekeeper for growth and division, Cell 88 (1997) 323–331.
[3] T. Kawabe, G2 checkpoint abrogators as anticancer drugs, Mol. Cancer Ther. 3 (2004) 513–519.
[4] J. Ptacek, G. Devgan, G. Michaud, H. Zhu, X. Zhu, J. Fasolo, H. Guo, G. Jona, A. Breitkreutz, R. Sopko, R.R. McCartney, M.C. Schmidt, N. Rachidi, S.J. Lee, A.S. Mah, L. Meng, M.J. Stark, D.F. Stern, C. De Virgilio, M. Tyers, B. Andrews, M. Gerstein, B. Schweitzer, P.F. Predki, M. Snyder, Global analysis of protein phosphorylation in yeast, Nature 438 (2005) 679–684.
[5] J.A. Ubersax, E.L. Woodbury, P.N. Quang, M. Paraz, J.D. Blethrow, K. Shah, K.M. Shokat, D.O. Morgan, Targets of the cyclin-dependent kinase Cdk1, Nature 425 (2003) 859–864.
[6] A. Lindqvist, V. Rodríguez-Bravo, R.H. Medema, The decision to enter mitosis: feedback and redundancy in the mitotic entry network, J. Cell Biol. 185 (2009) 193–202.
[7] S. Leijen, J.H. Beijnen, J.H. Schellens, Abrogation of the G2 checkpoint by inhibition of Wee-1 kinase results in sensitization of p53-deficient tumor cells to DNA-damaging agents, Curr. Clin. Pharmacol. 5 (2010) 186–191.
[8] J.M. Kreahling, J.Y. Gemmer, D. Reed, D. Letson, M. Bui, S. Altiok, MK1775, a selective Wee1 inhibitor, shows single-agent antitumor activity against sarcoma cells, Mol. Cancer Ther. 11 (2012) 174–182.
[9] P.C. De Witt Hamer, S.E. Mir, D. Noske, C.J.F. Van Noorden, T. Würdinger, WEE1 kinase targeting combined with DNA-damaging cancer therapy catalyzes mitotic catastrophe, Clin. Cancer Res. 17 (2011) 4200–4207.
[10] Y. Wang, S.J. Decker, J. Sebolt-Leopold, Knockdown of Chk1, Wee1 and Myt1 by RNA interference abrogates G2 checkpoint and induces apoptosis, Cancer Biol. Ther. 3 (2004) 305–313.
[11] C. Bruyère, S. Madonna, G.V. Goietsenoven, V. Mathieu, J. Dessolin, J.-L. Kraus, F. Lefranc, R. Kiss, JLK1486, a bis 8-hydroxyquinoline–substituted benzylamine, displays cytostatic effects in experimental gliomas through MyT1 and STAT1 activation and, to a lesser extent, PPARγ activation, Transl. Oncol. 4 (2011) 126–137.
[12] P.R. Mueller, T.R. Coleman, A. Kumagai, W.G. Dunphy, Myt1: a membrane-associated inhibitory kinase that phosphorylates Cdc2 on both threonine-14 and tyrosine-15, Science 270 (1995) 86–90.
[13] Y. Wang, J. Li, R.N. Booher, A. Kraker, T. Lawrence, W.R. Leopold, Y. Sun, Radiosensitization of p53 mutant cells by PD0166285, a novel G2 checkpoint abrogator, Cancer Res. 61 (2001) 8211–8217.
[14] O. Hashimoto, M. Shinkawa, T. Torimura, T. Nakamura, K. Selvendiran, M. Sakamoto, H. Koga, T. Ueno, M. Sata, Cell cycle regulation by the Wee1 inhibitor PD0166285, pyrido [2,3-d] pyimidine, in the B16 mouse melanoma cell line, BMC Cancer 6 (2006) 292.
[15] R.L. Panek, G.H. Lu, S.R. Klutchko, B.L. Batley, T.K. Dahring, J.M. Hamby, H. Hallak, A.M. Doherty, J.A. Keiser, In vitro pharmacological characterization of PD 166285, a new nanomolar potent and broadly active protein tyrosine kinase inhibitor, J. Pharmacol. Exp. Ther. 283 (1997) 1433–1444.
[16] B.-N. Zhou, S. Tang, R.K. Johnson, M.P. Mattern, J.S. Lazo, E.R. Sharlow, K. Harichd, D.G.I. Kingston, New glycolipid inhibitors of Myt1 kinase, Tetrahedron 61 (2005) 883–887.
[17] A. Rohe, F. Erdmann, C. Bäßler, K. Wichapong, W. Sippl, M. Schmidt, In vitro and in silico studies on substrate recognition and acceptance of human PKMYT1, a Cdk1 inhibitory kinase, Bioorg. Med. Chem. Lett. 22 (2012) 1219–1223.
[18] C.S. Lebakken, S.M. Riddle, U. Singh, W.J. Frazee, H.C. Eliason, Y. Gao, L.J. Reichling, B.D. Marks, K.W. Vogel, Development and applications of a broad-coverage, TR-FRET-based kinase binding assay platform, J. Biomol. Screen. 14 (2009) 924–935.
[19] C. Göllner, C. Philipp, B. Dobner, W. Sippl, M. Schmidt, First total synthesis of 1,2-dipalmitoyl-3-(*N*-palmitoyl-6′-amino-6′-deoxy-alpha-D-glucosyl)-sn-glycerol – a glycoglycerolipid of a marine alga with a high inhibitor activity against human Myt1-kinase, Carbohydr. Res. 344 (2009) 1628–1631.
[20] MOE 2010.10, Chemical Computing Group, Inc., Montreal, Canada, 2010.
[21] G. Jones, P. Willett, R.C. Glen, Molecular recognition of receptor-sites using a genetic algorithm with a description of desolvation, J. Mol. Biol. 245 (1995) 43–53.
[22] G. Jones, P. Willett, R.C. Glen, A.R. Leach, R. Taylor, Development and validation of a genetic algorithm for flexible docking, J. Mol. Biol. 267 (1997) 727–748.
[23] K. Wichapong, M. Lawson, S. Pianwanit, S. Kokpol, W. Sippl, Postprocessing of protein-ligand docking poses using linear response MM-PB/SA: application to Wee1 kinase inhibitors, J. Chem. Inf. Model. 50 (2010) 1574–1588.
[24] K. Wichapong, M. Lindner, S. Pianwanit, S. Kokpol, W. Sippl, Receptor-based 3D-QSAR studies of checkpoint Wee1 kinase inhibitors, Eur. J. Med. Chem. 44 (2009) 1383–1395.
[25] L. Munoz, R. Selig, Y.T. Yeung, C. Peifer, D. Hauser, S. Laufer, Fluorescence polarization binding assay to develop inhibitors of inactive p38 alpha mitogen-activated protein kinase, Anal. Biochem. 401 (2010) 125–133.
[26] O. Hantschel, U. Rix, G. Superti-Furga, Target spectrum of the BCR-ABL inhibitors imatinib, nilotinib and dasatinib, Leuk. Lymph. 49 (2008) 615–619.
[27] M.I. Davis, J.P. Hunt, S. Herrgard, P. Ciceri, L.M. Wodicka, G. Pallares, M. Hocker, D.K. Treiber, P.P. Zarrinkar, Comprehensive analysis of kinase inhibitor selectivity, Nat. Biotechnol. 29 (2011) 1046–1051.
[28] L. Stryer, D.D. Thomas, C.F. Meares, Diffusion-enhanced fluorescence energy transfer, Ann. Rev. Biophys. Bioeng. 11 (1982) 203–222.
[29] M. Bantscheff, D. Eberhard, Y. Abraham, S. Bastuck, M. Boesche, S. Hobson, T. Mathieson, J. Perrin, M. Raida, C. Rau, V. Reader, G. Sweetman, A. Bauer, T. Bouwmeester, C. Hopf, U. Kruse, G. Neubauer, N. Ramsden, J. Rick, B. Kuster, G. Drewes, Quantitative chemical proteomics reveals mechanisms of action of clinical ABL kinase inhibitors, Nat. Biotechnol. 25 (2007) 1035–1044.
[30] U. Rix, O. Hantschel, G. Dürnberger, L.L. Remsing Rix, M. Planyavsky, N.V. Fernbach, I. Kaupe, K.L. Bennett, P. Valent, J. Colinge, T. Köcher, G. Superti-Furga, Chemical proteomic profiles of the BCR-ABL inhibitors imatinib, nilotinib, and dasatinib reveal novel kinase and nonkinase targets, Blood 110 (2007) 4055–4063.
[31] T. O'Hare, D.K. Walters, E.P. Stoffregen, T. Jia, P.W. Manley, J. Mestan, S.W. Cowan-Jacob, F.Y. Lee, M.C. Heinrich, M.W.N. Deininger, B.J. Druker, In vitro activity of Bcr-Abl inhibitors AMN107 and BMS-354825 against clinically relevant imatinib-resistant Abl kinase domain mutants, Cancer Res. 65 (2005) 4500–4505.
[32] F. Zuccotto, E. Ardini, E. Casale, M. Angiolini, Through the "gatekeeper door": exploiting the active kinase conformation, J. Med. Chem. 53 (2010) 2681–2694.
[33] W. Davidson, L. Frego, G.W. Peet, R.R. Kroe, M.E. Labadia, S.M. Lukas, R.J. Snow, S. Jakes, C.A. Grygon, C. Pargellis, B.G. Werneburg, Discovery and characterization of a substrate selective p38 alpha inhibitor, Biochemistry US 43 (2004) 11658–11671.
[34] S.M. Lukas, R.R. Kroe, J. Wildeson, G.W. Peet, L. Frego, W. Davidson, R.H. Ingraham, C.A. Pargellis, M.E. Labadia, B.G. Werneburg, Catalysis and function of the p38 alpha circle MK2a signaling complex, Biochemistry US 43 (2004) 9950–9960.
[35] N.J. Wells, N. Watanabe, T. Tokusumi, W. Jiang, M.A. Verdecia, T. Hunter, The C-terminal domain of the Cdc2 inhibitory kinase Myt1 interacts with Cdc2 complexes and is required for inhibition of G(2)/M progression, J. Cell Sci. 112 (1999) 3361–3371.
[36] P.K. Smith, R.I. Krohn, G.T. Hermanson, A.K. Mallia, F.H. Gartner, M.D. Provenzano, E.K. Fujimoto, N.M. Goeke, B.J. Olson, D.C. Klenk, Measurement of protein using bicinchoninic acid, Anal. Biochem. 150 (1985) 76–85.